1521-0103/373/2/290–301$35.00
THE JOURNAL OF PHARMACOLOGY AND EXPERIMENTAL THERAPEUTICS

https://doi.org/10.1124/jpet.119.262790
J Pharmacol Exp Ther 373:290–301, May 2020

Distinct Regulation of σ_1 Receptor Multimerization by Its Agonists and Antagonists in Transfected Cells and Rat Liver Membranes[S]

Weimin Conrad Hong

Department of Pharmaceutical Sciences, Butler University, Indianapolis, Indiana

Received September 18, 2019; accepted February 4, 2020

ABSTRACT

Extensive studies have shown that the σ_1 receptor (σ_1R) interacts with and modulates the activity of multiple proteins with important biological functions. Recent crystal structures of σ_1R as a homotrimer differ from a dimer-tetramer model postulated earlier. It remains inconclusive whether ligand binding regulates σ_1R oligomerization. Here, novel nondenaturing gel methods and mutational analysis were used to examine σ_1R oligomerization. In transfected cells, σ_1R exhibited as multimers, dimers, and monomers. Overall, σ_1R agonists decreased, whereas σ_1R antagonists increased σ_1R multimers, suggesting that agonists and antagonists differentially affect the stability of σ_1R multimers. Endogenous σ_1R in rat liver membranes also showed similar regulation of oligomerization as in cells. Mutations at key residues lining the trimerization interface (Arg119, Asp195, Phe191, Trp136, and Gly91) abolished multimerization without disrupting dimerization. Intriguingly, truncation of the N terminus reduced σ_1R to apparent monomer. These results demonstrate that multiple domains play crucial roles in coordinating high-order quaternary organization of σ_1R. The E102Q σ_1R mutant implicated in juvenile amyotrophic lateral sclerosis formed dimers only, suggesting that dysregulation of σ_1R multimeric assembly may impair its function. Interestingly, oligomerization of σ_1R was pH-dependent and correlated with changes in [^{3}H](+)-pentazocine binding affinity and B_{max}. Combined with mutational analysis, it is reasoned that σ_1R multimers possess high-affinity and high-capacity [^{3}H](+)-pentazocine binding, whereas monomers likely lack binding. These results suggest that σ_1R may exist in interconvertible oligomeric states in a dynamic equilibrium. Further exploration of ligand-regulated σ_1R multimerization may provide novel approaches to modulate the function of σ_1R and its interacting proteins.

SIGNIFICANCE STATEMENT

The σ_1 receptor (σ_1R) modulates the activities of various partner proteins. Recently, crystal structures of σ_1R were elucidated as homotrimers. This study used novel nondenaturing gel methods to examine σ_1R oligomerization in transfected cells and rat liver membranes. Overall, agonist binding decreased, whereas antagonist binding increased σ_1R multimers, which comprised trimers and larger units. σ_1R multimers were shown to bind [^{3}H](+)-pentazocine with high affinity and high capacity. Furthermore, mutational analysis revealed a crucial role of its N-terminal domain in σ_1R multimerization.

Introduction

The σ receptor was named after the distinct behavioral signs induced by SKF10047 (*N*-allylnormetazocine) in a chronic spinal dog preparation (Martin et al., 1976). However, molecular cloning identified a 25-kDa membrane protein as the σ_1 receptor (σ_1R) (Hanner et al., 1996; Jbilo et al., 1997). Its sequence is highly conserved in evolution but distinct from opioid receptors, as originally proposed. Multiple alternative splice variants of σ_1R have been characterized (Pan et al., 2017), including an isoform lacking exon 3 (ΔE3), which encodes amino acids (aa) 119–149 (Ganapathy et al., 1999).

Extensive studies have shown that σ_1R can interact with and modulate the activity of a plethora of partner proteins, including channels, receptors, and transporters (Hayashi and Su, 2001, 2007; Aydar et al., 2002; Wu and Bowen, 2008; Carnally et al., 2010; Kim et al., 2010; Navarro et al., 2010; Balasuriya et al., 2012; Kourrich et al., 2013; Srivats et al., 2016; Hong et al., 2017; Sambo et al., 2017; Thomas et al., 2017)

This study was supported by Butler University Faculty Startup Fund and Holcomb Research Award (WCH). Portions of the work herein were presented at Experimental Biology (2017) and Society for Neuroscience (2017) meetings, and most data were presented at Experimental Biology (2019): FASEB J. 33, 1_supplement:665.11.
https://doi.org/10.1124/jpet.119.262790.
[S] This article has supplemental material available at jpet.aspetjournals.org.

ABBREVIATIONS: aa, amino acid; BD1008, *N*-[2-(3,4-dichlorophenyl)ethyl]-*N*-methyl-2-(1-pyrrolidinyl)ethylamine dihydrobromide; BD1047, *N*-[2-(3,4-dichlorophenyl)ethyl]-*N*-methyl-2-(dimethylamino)ethylamine dihydrobromide; BD1063, 1-[2-(3,4-dichlorophenyl)ethyl]-4-methylpiperazine dihydrochloride; CM304, 3-(2-(azepan-1-yl)ethyl)-6-(3-fluoropropyl)benzo[*d*]thiazol-2(3*H*)-one hydrochloride; DSP, dithiobis(succinimidyl propionate); DTG, 1,3-di-*o*-tolylguanidine; ΔE3, isoform lacking exon 3; FH-σ_1R, σ_1R with N-terminal FLAG and 2xHis_8 tags; GDN, glyco-diosgenin; HA, hemagglutinin; HEK293, human embryonic kidney 293; mAb, monoclonal antibody; MM, molecular mass; NE-100, 4-methoxy-3-(2-phenylethoxy)-*N*,*N*-dipropylbenzeneethanamine monohydrochloride; NT, N terminal; PFO, perfluorooctanoic acid; PRE-084, 2-(4-morpholinethyl) 1-phenylcyclohexanecarboxylate hydrochloride; σ_1R, σ_1 receptor; RT, room temperature; SKF10047, *N*-allylnormetazocine; SLS, sodium lauroyl sarcosinate; SPB, sucrose-phosphate buffer; TM, transmembrane domain; WT, wild type.

that play important roles in cellular homeostasis and neuronal signaling. The majority of σ_1R protein is located in endoplasmic reticulum, particularly mitochondria-associated endoplasmic reticulum membranes (Hayashi and Su, 2007), which are critical sites to modulate energy balance, calcium regulation, and stress response. Several σ_1R mutations have recently been implicated in juvenile amyotrophic lateral sclerosis and distal hereditary motor neuropathies. Molecular mechanisms underlying such motor neuron deficits have been studied intensively, and aberrant σ_1R expression and function appear to be crucial in these conditions (Al-Saif et al., 2011; Bernard-Marissal et al., 2015; Li et al., 2015; Gregianin et al., 2016; Watanabe et al., 2016; Dreser et al., 2017).

Many clinical drugs and synthetic compounds with diverse structures exhibit varying affinities for σ_1R (Matsumoto, 2007; Cobos et al., 2008; Maurice and Su, 2009; Chu and Ruoho, 2016) and appear to share a limited pharmacophore consensus (Walker et al., 1990; Ablordeppey and Glennon, 2007; Newman and Coop, 2007; Weber and Wunsch, 2017). Several candidate endogenous ligands have been proposed over the years, including neurosteroids (Su et al., 1988; Bergeron et al., 1996), sphingosine (Ramachandran et al., 2009), and *N*,*N*-dimethyltryptamine (Fontanilla et al., 2009), but these hypotheses have not been conclusively confirmed. Traditionally σ_1R ligands have been classified as agonists or antagonists, depending upon whether they produce or block certain cellular, physiologic, or behavioral responses. Although affinities of these ligands for σ_1R have been extensively studied using traditional binding techniques, molecular mechanisms for agonists or antagonists to induce distinct changes of σ_1R remain largely unknown.

The ability to modulate σ_1R function with different ligands has made it an attractive target for developing novel therapeutic strategies. It has been shown that σ_1R agonists have ameliorative effects in several animal models of neurodegenerative disorders, such as Alzheimer's disease (Lahmy et al., 2013; Maurice and Goguadze, 2017; Ryskamp et al., 2019), Parkinson's disease (Francardo et al., 2014), Huntington's disease (Ryskamp et al., 2017), and retinal degeneration (Wang et al., 2016), whereas σ_1R antagonists have pain-relief effects (Merlos et al., 2017). Accumulating evidence also suggests that σ receptors are critically involved in cellular adaptive mechanisms elicited by psychostimulants (Cai et al., 2017; Katz et al., 2017) and alcohol (Sabino and Cottone, 2017). Therapeutic potentials of σ_1R antagonists have been explored in rodent models of cocaine or methamphetamine addiction (Hiranita et al., 2011; Robson et al., 2014; Sambo et al., 2017).

Whether σ_1R possesses one or two transmembrane domains (TMs) has been controversial (Hanner et al., 1996; Aydar et al., 2002; Hayashi and Su, 2007). In recent years, atomic force microscopy and solution NMR methods were employed to explore σ_1R structures (Carnally et al., 2010; Balasuriya et al., 2012; Ortega-Roldan et al., 2013). Breakthrough on the crystal structures of σ_1R has elucidated its homotrimer organization, with each protomer containing a single TM and a cytoplasmic ligand-binding pocket (Schmidt et al., 2016). Such structural architecture differs from a dimer-tetramer model postulated by early work (Chu and Ruoho, 2016). Furthermore, crystal structures of σ_1R bound with agonist (+)-pentazocine or antagonist haloperidol showed similar homotrimer organization with limited conformational rearrangement (Schmidt et al., 2018), suggesting that trimers may be the lowest free-energy state of σ_1R during crystallization. It remains unclear whether ligand binding affects the native high-order organization of σ_1R. This study examined σ_1R oligomerization using molecular, biochemical, and pharmacological techniques. The results show that multiple domains on σ_1R coordinate its multimerization. Furthermore, agonists and antagonists dynamically regulate σ_1R oligomerization in distinct manners, and quaternary structures of σ_1R significantly impact ligand binding.

Materials and Methods

Chemicals, Radioligands, and Antibodies. Sources of reagents are as follows: (−)-Cocaine HCl, (+)-pentazocine succinate, and (+)-SKF10047 were obtained from National Institute on Drug Abuse Drug Supply Program; PRE-084 was obtained from Tocris (Minneapolis, MN); 1,3-di-*o*-tolylguanidine (DTG), BD1008, BD1047, BD1063, and NE-100 were gifts from Dr. Jonathan L. Katz; CM304 was a gift from Dr. Christopher R. McCurdy; *d*-erythro-sphingosine, dehydroepiandrosterone, and haloperidol were obtained from Cayman chemicals (Ann Arbor, MI); BCA protein kit was obtained from Pierce (Rockford, IL); perfluorooctanoic acid (PFO) and sodium lauroyl sarcosinate (SLS) were obtained from TCI America (Portland, OR); glyco-diosgenin (GDN) was obtained from Anatrace (Maumee, OH); all other chemicals were obtained from Sigma-Aldrich (St. Louis, MO) or Fisher Scientific (Pittsburgh, PA); glutathione-conjugated Sepharose beads were obtained from GE Healthcare (Pittsburgh, PA); [^{3}H](+)-pentazocine (NET-1056, 26.9 Ci/mmol) was obtained from Perkin Elmer (Boston, MA); anti-FLAG rat mAb L5, anti-HA mAb HA11, anti-Myc mAb 9E10, and horseradish peroxidase–conjugated secondary antibodies were obtained from Biolegend (San Diego, CA); and anti-σ_1R mAb clone B5 was obtained from Santa Cruz Biotechnology (Santa Cruz, CA).

DNA Subcloning and Stable Expression Cell Lines. The coding sequences of human σ_1R cDNA were subcloned into cytomegalovirus promoter-based mammalian expression plasmids expressing N-terminal fusion of HA, Myc, or FLAG-2xHis_8 tags (Hong et al., 2017). σ_1R mutants were generated using the QuikChange method, verified by standard DNA-sequencing procedures. Plasmids DNA were linearized and transfected into cells using TransIT LT1 reagent (Mirus Bio, Madison, WI) to isolate G418-resistant clones. Alternatively, cells were transiently transfected using PolyJet (SignaGen, Rockville, MD). Cells were then cultured in Dulbecco's modified Eagle's medium with 10% FBS (Sigma) and penicillin-streptomycin in humidified incubators with 5% CO_2 at 37°C. G418 (0.5 mg/ml) was included for stable lines, and expression of σ_1R was verified by immunoblot using antibodies against σ_1R or epitope tags.

Rat Liver Membrane Preparations. Fresh liver tissues from mixed sex Sprague-Dawley rats (BioIVT, Hicksville, NY) were rinsed with cold PBS, cut into small pieces with a razor blade, washed with ice-cold sucrose-phosphate buffer (SPB) (0.32 M sucrose, 7.74 mM Na_2HPO_4, 2.26 mM NaH_2PO_4, pH 7.4), and resuspended in SPB (1:10 ratio, w/v in grams:milliliters). Tissues were homogenized in a glass homogenizer with a motor-driven Teflon pestle at 2000 rpm for 20 strokes and centrifuged at 1000*g* for 10 minutes at 4°C. The supernatant was centrifuged at 10,000*g* for 10 minutes at 4°C. The resulting pellet was resuspended in SPB by vortexing (1:4 w:v), aliquoted, and frozen in liquid N_2.

Drug Treatment. Confluent cells in 12-well plates were incubated at 37°C in culture medium with σ_1R ligands for 1 hour (Fig. 1, A–C; Fig. 2) or antagonists for 0.5 hours, which was followed by agonist for 1 hour (Fig. 1, D and E). Cells were then washed with cold PBS with 0.1 mM $CaCl_2$ and 1 mM $MgCl_2$, harvested, and incubated with GDN-Tris lysis buffer (0.1% GDN, NaCl 150 mM, EDTA 1 mM, Tris 10 mM, pH 7.5, and protease inhibitors) for 2 hours at 4°C, and this was followed by centrifugation at 20,000*g* for 20 minutes. The resulting supernatants were used as GDN lysates. In Fig. 3, GDN

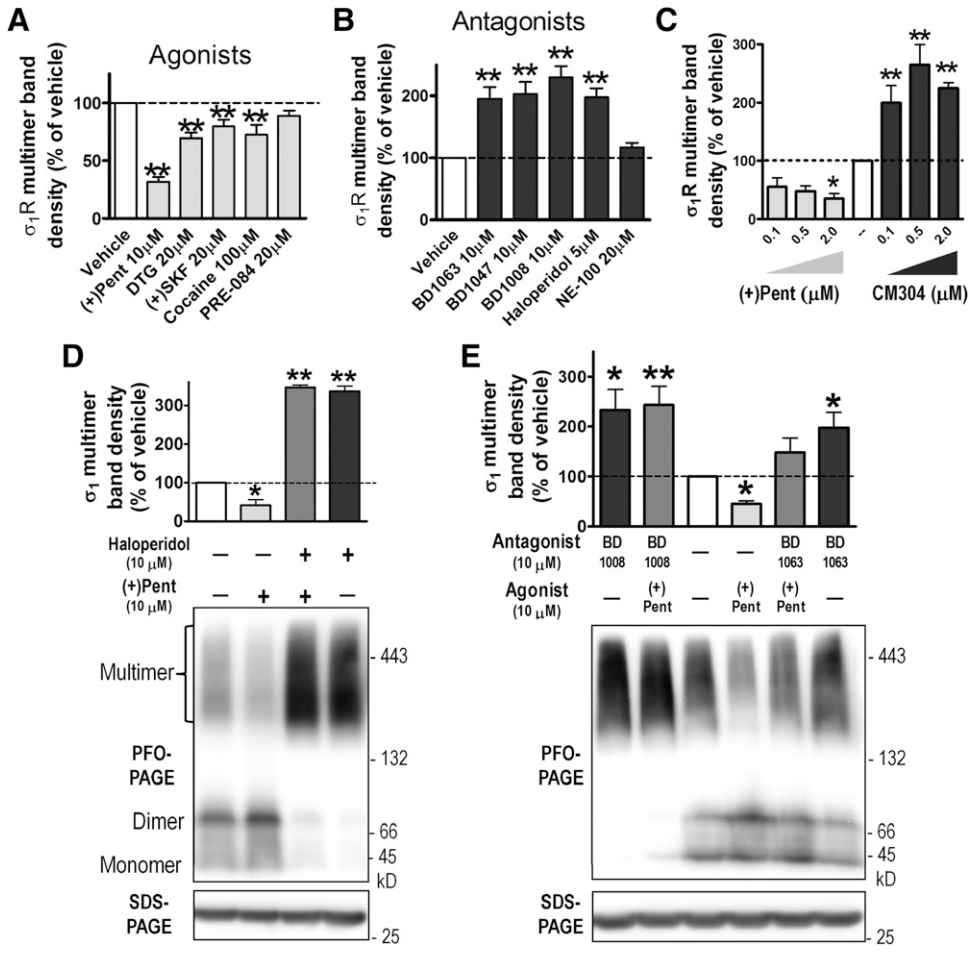

Fig. 1. Distinct effects on σ_1R multimerization by agonists or antagonists in PFO-PAGE. HEK293 cells stably transfected with FH-σ_1R were treated with drugs at 37°C [in (A–C): agonists or antagonists for 1 hour; in (D and E): antagonists 0.5 hours, then (+)-pentazocine 1 hour], lysed in GDN-Tris buffer, and run in PFO-PAGE. (A) Agonists decreased high-MM multimers. (B) Antagonists increased high-MM multimers. (C) Dose-dependent effects by agonist (+)-pentazocine or antagonist CM304. (D and E) Interaction of agonist and antagonists on σ_1R multimerization, with representative immunoblots. All panels show column graphs (mean ± S.E.M.) from multiple experiments (n): (A), n = 4–7; (B), n = 4–11; (C), n = 3–6; (D), n = 3; (E), n = 4–7. $^*P < 0.05$, $^{**}P < 0.01$, one-way ANOVA and post-hoc Dunnett's test, compared with vehicle. kD, kDa; (+)Pent, (+)-pentazocine; (+)SKF, (+)-SKF10047.

lysates of cells were incubated with drugs overnight on ice before gel analysis.

Liver membranes were thawed and divided into equal portions in microcentrifuge tubes. Drugs were added to tubes and incubated at 37°C for 2 hours. Tubes were centrifuged at 15,000g for 10 minutes at 4°C, and the pellets were lysed similarly as cells, except with the GDN-HEPES lysis buffer (20 mM HEPES was used to replace Tris).

Analysis of σ_1R Multimeric States by PFO-PAGE and SLS-PAGE. GDN lysates were mixed with an equal volume of 2× sample buffer (40% glycerol, bromophenol blue 0.005%, Tris 100 mM, 8% PFO, or 4% SLS, pH 7.5) to a final concentration of 4% PFO or 2% SLS and heated at 37°C for 10 minutes. Samples were run in 5%–15% polyacrylamide Tris-glycine gels (running buffer: 0.1% PFO or 0.1% SLS, 25 mM Tris, 192 mM glycine, pH 8.3). Proteins were transferred to polyvinylidene difluoride membranes and immunoblotted with FLAG, HA, or σ_1R antibodies. Chemiluminescent signals were captured with a MultiImage III device (Alpha Innotech, San Leandro, CA) as digital TIFF images without pixel saturation. Integrated densities of bands were quantified using the NIH ImageJ software and normalized to percent of vehicle. The following proteins (from Sigma-Aldrich) were mixed with PFO or SLS sample buffer and used as molecular standards: egg white lysozyme (14 kDa), ovalbumin (45 kDa), bovine serum albumin (66 kDa monomer, 132 kDa dimer), bovine liver catalase (240 kDa), and equine apoferritin (443 kDa). Because of stable expression of tagged σ_1R, variances of σ_1R levels in cell lysates within each experiment were usually minimal. GDN lysates were also mixed with 4 × SDS sample buffer, heated at 85°C for 10 minutes, run in SDS-PAGE, transferred, and blotted to verify equal loading of total σ_1R.

Crosslinking of σ_1R. GDN-HEPES lysates from cells or rat liver were incubated with 0.2 to 1 mM dithiobis(succinimidyl propionate) (DSP) (a bifunctional, primary amine-reactive crosslinker with a cleavable disulfide bond) at 25°C for 1 hour, mixed with SDS sample buffer without dithiothreitol, heated at 85°C for 10 minutes, and run in SDS-PAGE. A parallel set of lysates were treated with DSP and further incubated with 20 mM tris(2-carboxyethyl)phosphine at 25°C for 0.5 hours to reduce the disulfide bond in DSP.

[^{3}H](+)-Pentazocine Binding in GDN-Solubilized Cell Lysates. Transfected human embryonic kidney 293 (HEK293) cells were harvested from 150-mm dishes, lysed in GDN-Tris buffer at 4°C with gentle shaking, and centrifuged at 20,000g for 30 minutes. Supernatants were collected and adjusted to final pH values of approximately 6, 7.5, or 9 by diluting with appropriate combinations of 1 M solutions of Tris-HCl (pH 7.5), Tris base (pH 10.4), or Tris-HCl (pH 4.7) to final 10 mM Tris, and GDN was supplemented to 0.02%. Binding reactions were set up in polystryrene tubes containing 200 μl diluted lysates and 50 μl drugs (5 nM [^{3}H](+)-pentazocine and various concentrations of competing ligands). After overnight incubation on ice, 4 ml ice-cold Tris buffer (10 mM, pH 7.5) was added to each tube, and the mixture was rapidly filtrated onto 0.05% polyethylenimine-soaked GF/B filter papers using an M-24 harvester (Brandel Instruments, Gaithersburg, MD), and this was followed by three washes of 3 ml Tris buffer. Dried filters were soaked with 3 ml liquid scintillation cocktail overnight and measured for radioactivity using a Tri-Carb 2900TR liquid scintillation counter (Perkin Elmer) at 45% efficiency. Nonspecific binding measured in the presence of 10 μM haloperidol was generally <10% of total binding for wild-type (WT) σ_1R and subtracted from total counts to obtain specific binding. Data were analyzed using GraphPad Prism (San Diego, CA) for nonlinear regression to derive B_{max} or K_d values.

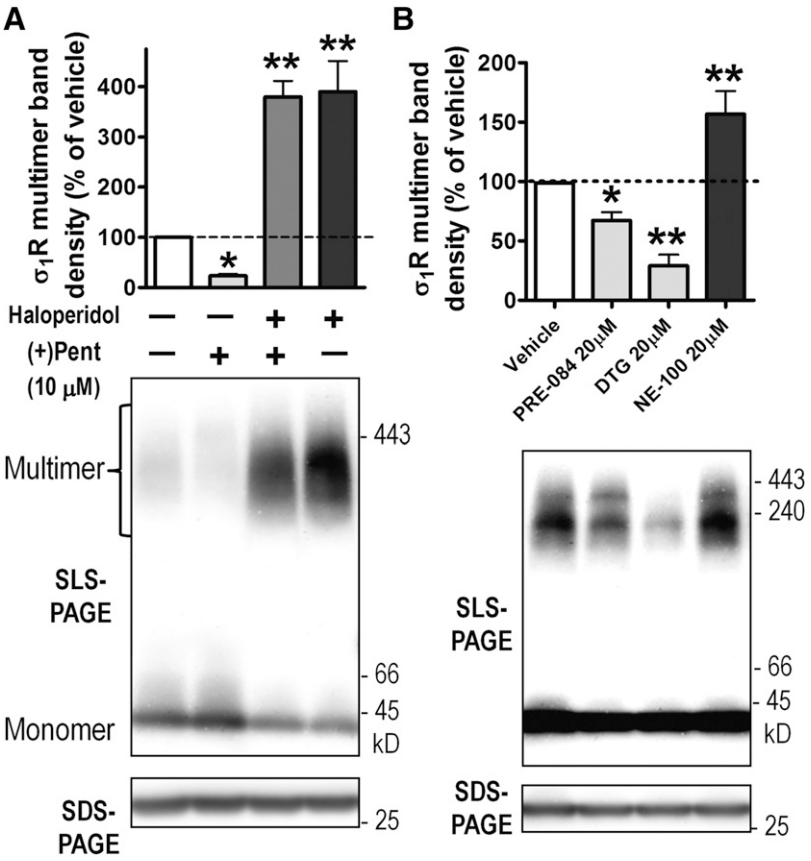

Fig. 2. Distinct effects on σ_1R multimerization by agonists or antagonists detected with SLS-PAGE, which showed a higher sensitivity than PFO-PAGE. (A and B) Samples from FH-σ_1R cells pretreated with drugs as in Fig. 1. Representative immunoblots and summary column graphs (mean ± S.E.M.) from multiple experiments: (A), n = 3–6; (B), n = 4–8. *$P < 0.05$; **$P < 0.01$, one-way ANOVA and Fisher's least significant difference test, compared with vehicle. kD, kDa; (+)Pent, (+)-pentazocine.

Results

Previously, we reported a nondenaturing gel method that detected σ_1R monomer, dimer, or high molecular mass (MM) multimers based on their apparent electrophoretic mobility. The proportion of σ_1R multimers was decreased by the agonist (+)-pentazocine but increased by the antagonist CM304 (Hong et al., 2017). In this assay, during gel electrophoresis, SDS was replaced by PFO, a mild detergent shown to preserve protein oligomers (Ramjeesingh et al., 1999; Penna et al., 2008).

After literature review, σ_1R drugs that are well-characterized as agonists or antagonists were selected for this study. HEK293 cells were stably transfected with the WT human σ_1R containing N-terminal FLAG and 2xHis_8 tags (FH-σ_1R) (predicted MM of 32 kDa: 25 kDa σ_1R + 7 kDa tags with linker) and cultured to confluency in multiwell plates to minimize samples variability. Cells then were incubated with drugs in culture medium at 37°C for 1 hour, washed, and solubilized using a mild detergent, GDN. Lysates were run in PFO-PAGE and immunoblotted with FLAG antibodies. The two lower-MM bands matched the estimated size of σ_1R monomer (comprising one σ_1R polypeptide or protomer) and dimer (comprising two protomers). High-MM diffused bands likely represented multiple forms apparently larger than trimers (three promoters), and are thus termed as "multimers" in this study. Oligomerization of σ_1R is defined as assembly from monomers to any form containing at least two σ_1R protomers, whereas multimerization specifically refers to formation of σ_1R complexes containing three and more protomers.

σ_1R agonists (+)-pentazocine, DTG, (+)-SKF10047, and cocaine all significantly decreased σ_1R multimer band density, with (+)-pentazocine producing largest effect (32% ± 4% of vehicle, Fig. 1A). In contrast, σ_1R antagonists (BD1063, BD1047, BD1008, and haloperidol) all significantly increased the band density of σ_1R multimers above 2-fold of that in vehicle (Fig. 1B), resembling effects of CM304. Because they mostly have nanomolar affinities for σ_1R, low micromolar concentrations of these drugs were likely sufficient to permeate through cell membranes and occupy most of intracellular σ_1R sites during incubation and induce significant effects on its multimerization.

Distinct effects of (+)-pentazocine were dose-dependent, ranging from 0.1 to 2 μM (Fig. 1C). Further, pre-exposure of antagonists (haloperidol, BD1008, or BD1063) in these cells for 0.5 hours blocked (+)-pentazocine's effects (Fig. 1, D and E). Notably, these drugs did not change the total pool of σ_1R (shown in SDS-PAGE) but altered the proportion of multimers to dimers and monomers. Dose-dependent effects of haloperidol (0.1–1 μM) on reversing (+)-pentazocine's effects were also shown in PFO-PAGE (Yano et al., 2018). These data showed that generally σ_1R agonists and antagonists induced opposite effects on σ_1R multimerization. Effects by PRE-084 and NE-100 were consistent as agonist or antagonist, respectively, although these were not statistically significant.

Other mild detergents were then explored. If lysates were mixed with 2% sodium deoxycholate, only high-MM σ_1R multimeric bands were seen (unpublished data). Fortuitously, replacing 4% PFO with 2% SLS (Reichel, 2012), an ionic detergent less stringent than SDS, yielded remarkable results. σ_1R mainly showed as monomer and multimer bands, with the dimer band largely absent. Consistent with results in PFO-PAGE, (+)-pentazocine decreased, whereas haloperidol

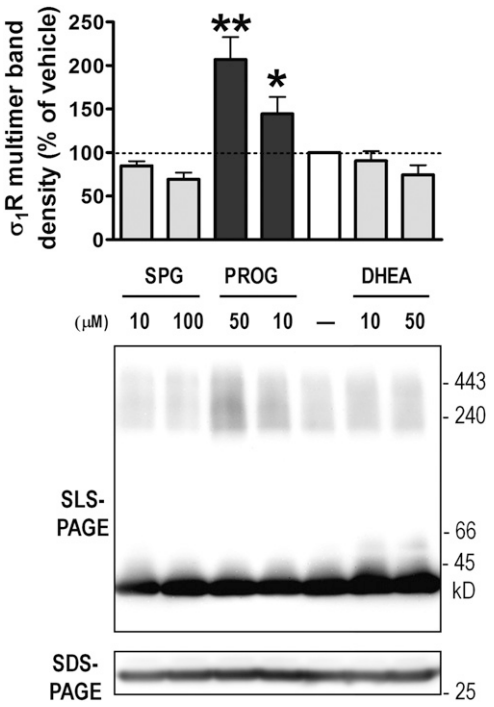

Fig. 3. Effects of putative endogenous ligands on σ_1R multimerization. GDN lysates from drug-naïve FH-σ_1R cells were incubated with ligands on ice overnight and then run in SLS-PAGE. Representative immunoblots and summary (mean ± S.E.M.) from n = 4–8 experiments. *$P < 0.05$; **$P < 0.01$, one-way ANOVA and Fisher's least significant difference test, compared with vehicle. DHEA, dehydroepiandrosterone; kD, kDa; PROG, progesterone; SPG, *d*-erythro-sphingosine.

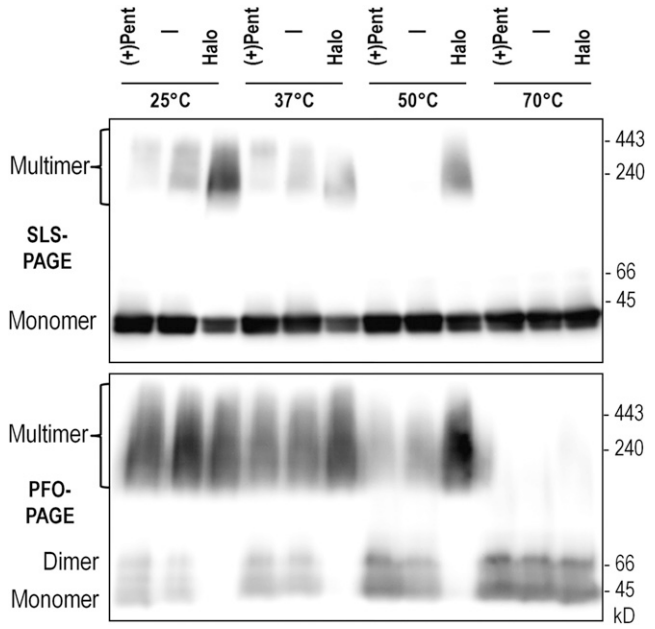

Fig. 4. (+)-Pentazocine and haloperidol differentially affected the thermostability of σ_1R multimers. FH-σ_1R cells were treated with vehicle or drugs (10 μM) at 37°C for 1 hour before lysis. Cell lysates were mixed with 2× concentrated PFO or SLS loading buffer; incubated for 10 minutes at 25, 37, 50, and 70°C; run in PFO-PAGE or SLS-PAGE; and immunoblotted with Flag antibody. Representative blots from n = 3 experiments. Halo, haloperidol; kD, kDa; (+)Pent, (+)-pentazocine.

increased σ_1R multimers in SLS-PAGE (Fig. 2A). However, this assay had a higher sensitivity. Haloperidol increased σ_1R multimer band densities to approximately 4-fold of vehicle, and (+)-pentazocine decreased σ_1R multimer bands to 23% ± 4% of vehicle. Furthermore, in SLS-PAGE, significant effects on σ_1R multimeric band densities by NE-100 (157% ± 19% of control) and PRE-084 (67% ± 7% of control, Fig. 2B) were revealed. Interestingly, σ_1R multimers appeared as multiple high-MM smeared bands but were apparently larger than 100 kDa, suggesting that transfected σ_1R might exist in multimeric forms larger than homotrimers.

Because most σ_1R is located on intracellular membranes, during incubation, drugs permeated through cell membranes to bind σ_1R, and most likely they remained bound to σ_1R during cell lysis since (+)-pentazocine and haloperidol were shown to dissociate very slowly from σ_1R (dissociation $t_{1/2} >$ 3 hours) using traditional radioligand off-rate method (Bowen et al., 1993) or scintillation proximity assay (Schmidt et al., 2018). Furthermore, if lysates from drug-naïve cells were incubated with drugs overnight on ice, similar effects as those in preincubation were seen (Supplemental Fig. 1). Lastly, FH-σ_1R cell lysates exhibited robust binding of [^{3}H](+)-pentazocine (Fig. 7), suggesting that GDN solubilization, to a large extent, preserved active conformations of σ_1R capable of ligand binding.

These features facilitated examination of effects by potential endogenous ligands of σ_1R. Several candidates have been proposed, including progesterone (Su et al., 1988), dehydroepiandrosterone (Bergeron et al., 1996), and *d*-erythro-sphingosine (Ramachandran et al., 2009). Because of their limited water solubility, it was difficult to incubate cells at concentrations close to their binding affinities for σ_1R (high nanomolars to low micromolars). However, these lipids could be dissolved in ethanol at 10 mM and then mixed with GDN-solubilized FH-σ_1R cell lysates to achieve final concentrations of 10–100 μM. After overnight incubation on ice, lysates were then subjected to SLS-PAGE. Compared with vehicle treatment (0.5% ethanol), progesterone (10 and 50 μM) significantly increased σ_1R multimers (144% ± 19% and 207% ± 26% of vehicle, Fig. 3). Dehydroepiandrosterone and *d*-erythro-sphingosine appeared to induce a slight, dose-dependent decrease of σ_1R multimers, albeit not statistically significant. Another proposed endogenous ligand for σ_1R, *N*,*N*-dimethyltryptamine (Fontanilla et al., 2009), as a Schedule I controlled substance, is not available at the current institution and was not tested.

In PFO-PAGE and SLS-PAGE, GDN lysates typically were mixed with PFO or SLS and heated at 37°C for 10 minutes before gel analysis. Distinct effects of agonists and antagonists suggest that they differentially affect the stability of σ_1R multimers. To test this idea, GDN lysates from drug-treated FH-σ_1R cells were mixed with PFO or SLS loading buffer and incubated at four different temperatures (25, 37, 50, and 70°C) for 10 minutes before being analyzed in PFO-PAGE or SLS-PAGE. The proportion of σ_1R multimer was gradually decreased by rising temperatures before disappearing at 70°C. Compared with vehicle, at each condition, (+)-pentazocine consistently decreased, whereas haloperidol increased σ_1R multimers (Fig. 4). Even at 50°C, haloperidol clearly protected σ_1R multimers. Hence, the antagonist haloperidol appeared to enhance the thermostability of σ_1R multimers, whereas agonist (+)-pentazocine had opposite effects.

Several approaches were used to allay the concern that epitope-tagged σ_1Rs in transfected cells may have different quaternary organizations than native σ_1R. First, effects of different epitope tags in stably transfected HEK293 cells were compared. Distinct effects by (+)-pentazocine and BD1008 were preserved for HA-tagged σ_1R (Supplemental Fig. 2A) in PFO-PAGE. Second, HEK293 cells were transiently transfected to express FH-σ_1R at different levels. Regardless of high or low expression, BD1008 increased, whereas (+)-pentazocine decreased FH-σ_1R multimers in SLS-PAGE and PFO-PAGE (Supplemental Fig. 2B).

Furthermore, whether drugs affect endogenous σ_1R multimerization was examined in rat liver tissues, where σ_1R is enriched (McCann and Su, 1991). Rat liver membranes were incubated with drugs and solubilized with GDN lysis buffer. Lysates were then subjected to nondenaturing gel analysis, and immunoblotted with a mouse monoclonal antibody for σ_1R (clone B5; Santa Cruz Biotechnology). Different from cell lysates, in PFO-PAGE σ_1R were detected as almost exclusively high-MM smear bands, very faint signals of dimer bands based on apparent electrophoretic mobility, and absence of monomers. Compared with vehicle, (+)-pentazocine and BD1008 appeared to increase or decrease the dimer signal, respectively (Fig. 5A). In SDS-PAGE, σ_1R in rat liver lysates only showed as a single band of 25 kDa if lysates were mixed with SDS (final 1%) and heated to 85°C. If the mixture was incubated at room temperature (RT) for 1 hour, a faint band near 75 kDa appeared in BD1008-treated samples (Fig. 5B). The apparent MM of this band was consistent with a σ_1R trimer, suggesting that in liver membranes, BD1008-induced σ_1R trimers were stable enough to partially resist SDS treatment at RT. Absence of nonspecific bands validated this antibody for detecting native σ_1R.

Most importantly, drug effects were convincingly shown when samples were run in SLS-PAGE (Fig. 5C). Compared with vehicle, (+)-pentazocine significantly decreased the proportion of multimers in total σ_1R proteins, with a concomitant increase in σ_1R monomers. In contrast, BD1008 had a significant effect opposite to (+)-pentazocine (Fig. 5, C and D). These drug effects were very similar to those seen in transfected HEK293 cells (Fig. 2), but the difference in σ_1R multimer MM was worth noting. In rat liver lysates, these bands appeared to range from approximately 70 kDa (possible trimer) to beyond 400 kDa, with the highest density near approximately 100 kDa, but those from cells appeared to have larger MM sizes (Fig. 2). This suggests that high-order quaternary organization of native or heterologously overexpressed σ_1R might not be the same, but drug effects on σ_1R multimerization were preserved overall. It should be cautioned that MM estimation of these bands was limited because of the nature of these gels.

Crosslinking assays were done to validate the presence of σ_1R multimers. DSP is a bifunctional crosslinker that selectively reacts with primary amines with a cleavable disulfide bond in its 12-Å spacer arm. DSP crosslinking in rat liver GDN lysates induced a 50-kDa band after nonreducing SDS-PAGE, which disappeared with tris(2-carboxyethyl)phosphine treatment to reduce disulfide bonds (Supplemental Fig. 3A). Because rat σ_1R has a sole lysine (Lys142), with its side chain solvent-accessible, based on human σ_1R crystal structures (Schmidt et al., 2016), the 50-kDa band was most likely a dimer formed through crosslinking at Lys142. FH-σ_1R has three more lysine residues in its epitope and linker. DSP

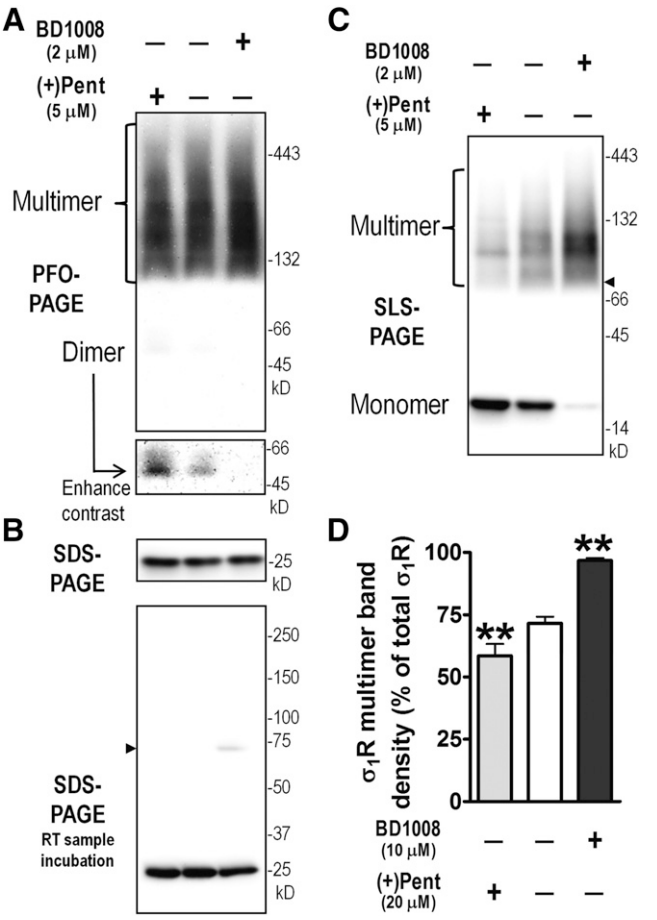

Fig. 5. Analysis of drugs' effects on σ_1R multimerization in rat liver membranes. Rat liver membranes were treated with drugs for 2 hours at 37°C, followed by lysis with GDN-HEPES buffer. (A) In PFO-PAGE, σ_1R predominantly showed as smear bands above approximately 100 kDa, whereas a very weak dimer band appeared to be increased after (+)-pentazocine treatment and decreased by BD1008. (B) In SDS-PAGE, only 25 kDa σ_1R monomer was present if lysates were heated with SDS. However, σ_1R trimer band (75 kDa, ▶) was revealed in BD1008-treated samples after RT incubation with SDS. (C) Significant effects by (+)-pentazocine and BD1008 in SLS-PAGE. σ_1R multimer bands ranged from approximately 70 kDa (possible trimer, ▶) to above 300 kDa, with most density near 100 kDa. (D) Summary graph showed σ_1R multimer band densities as % of total σ_1R (mean ± S.E.M., $n = 5$ experiments) in SLS-PAGE. $^{**}P < 0.01$, one-way ANOVA and post hoc Dunnett's test. kD, kDa; (+)Pent, (+)-pentazocine.

crosslinking induced multiple high-MM bands. Beside a clear dimer band, two discernible bands were detected at positions corresponding to trimer and tetramer as well as smeared bands above 150 kDa (Supplemental Fig. 3B). These data suggest that in transfected cells, trimers of σ_1R could exist, yet they might undergo further assembly; thus, trimer bands were not detected in nondenaturing gels (Figs. 1 and 2).

Recent breakthrough on crystal structures of σ_1R shed new light on key residues mediating homotrimer formation (Schmidt et al., 2016). Mutants of σ_1R at these pivotal positions were examined in nondenaturing gels. In WT σ_1R, the benzyl side chains of Phe191 in three protomers form aromatic interaction with each other (Fig. 6A). Mutation of Phe191 to Gly (F191G) removed this interaction and abolished σ_1R multimerization but appeared to retain dimerization (lane 1, Fig. 6B). The hydrophobic side chain of Trp136 in WT σ_1R interacts extensively with several residues in the

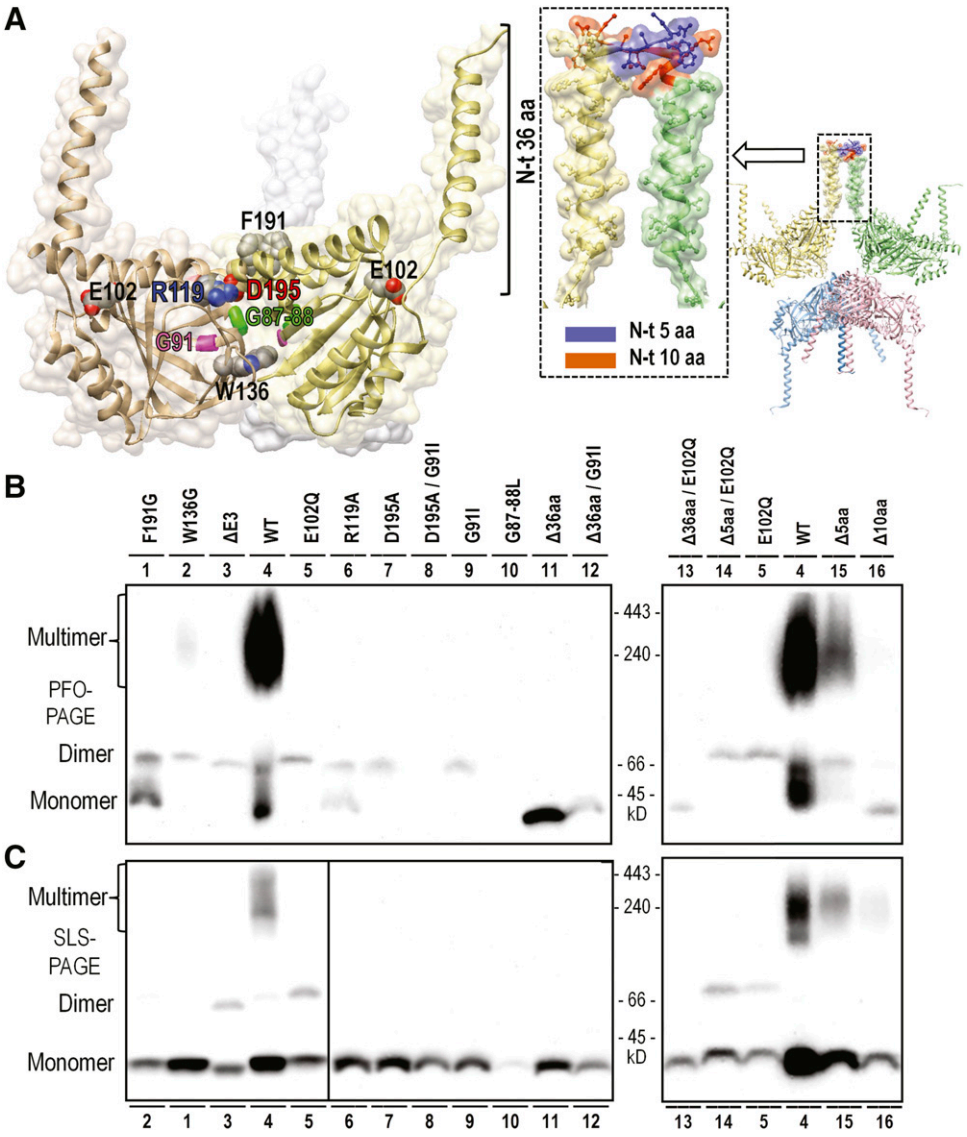

Fig. 6. Mutational analyses show that multiple domains on σ_1R are critical for its multimerization. (A) Structure cartoons of σ_1R with mutated residues annotated. Left: side view of σ_1R homotrimer, with transparent surface presentation and peptide backbone in ribbon. Side chains of specific residues are highlighted. Right: unit cell organization of four σ_1R homotrimers in its crystal structure. Zoomed view: parallel alignment of N-terminal 36 aa from two protomers in neighboring homotrimers. Cartoons are based on Protein Data Bank code 5HK1 (Schmidt et al., 2016) and generated using UCSF Chimera software. (B and C) Distinct electrophoretic migration pattern of σ_1R constructs. GDN lysates from HEK293 cells transiently transfected with WT and mutant FH-σ_1R were run in PFO-PAGE and SLS-PAGE, which was followed by immunoblot detection using Flag antibodies. Representative blots from $n > 3$ experiments. Constructs are numbered and aligned in both blots, except lanes 1 and 2 were switched in SLS-PAGE. Lack of signals in lanes 8 and 10 of PFO-PAGE was likely due to low expression of these mutants. kD, kDa.

neighboring protomer. Substitution of Trp136 with Gly (W136G) showed severely reduced multimerization and a dimer but no monomer band (lane 2, Fig. 6B). Crystal structures show that Arg119 and His116 of a WT protomer form a network of hydrogen bonds with Asp195 and Thr198 of its neighboring protomers, which is critical in maintaining trimerization interface. Alanine substitution at either position (R119A or D195A) abolished multimerization but preserved dimerization, as observed in PFO-PAGE (lane 6 and 7, Fig. 6B). A σ_1R splice variant skipping exon3 (ΔE3, encoding aa 119–149) showed only as dimer but not multimer in PFO-PAGE (lane 3, Fig. 6B), confirming the essential roles of Arg119 and Trp136 in protomer multimerization.

Genetic studies have identified several σ_1R mutants that are implicated in neurodegenerative diseases with motor neuron deficits. The Glu102Gln (E102Q) mutant is associated with juvenile amyotrophic lateral sclerosis (Al-Saif et al., 2011). In contrast with WT σ_1R, it failed to form multimers but appeared as dimer exclusively in PFO-PAGE (lane 5, Fig. 6B). The WT σ_1R showed signals of strong monomer, weak multimer, and very faint dimer in SLS-PAGE, but the E102Q mutant and ΔE3 variant exhibited strong dimer signals, suggesting that such sequence alterations abolished σ_1R multimerization but promoted dimer formation (lane 3 and 5, Fig. 6C). Another disease mutant, Glu138Gln (E138Q) (Gregianin et al., 2016), also appeared to have impaired multimerization (unpublished data).

A recent study reported an important role of a GXXXG motif (residues 87–91) in oligomerization of σ_1R. Mutations replacing glycine with residues containing bulky aliphatic side chains appeared to abolish σ_1R multimers but preserve dimers and monomers, as examined in size-exclusion chromatography using σ_1R mutants expressed in *Escherichia coli* (Gromek et al., 2014). Two such mutants, Gly91Ile (G91I) and Gly87Leu-Gly88Leu (G87-88L), had low expression levels in transfected cells, as similarly observed in bacterial expression. The G91I mutant showed only as dimer, without multimer or monomer, in PFO-PAGE (lane 9, Fig. 6B). Weak signals of G87-88L were detected in SLS-PAGE, whereas in PFO-PAGE, little if no signals were seen. Overall, these results confirmed the importance of key residues at trimerization interface and the GXXXG motif in σ_1R multimerization.

Further mutational analyses were conducted to explore the dimeric interface. Very weak expression of double mutants (D195A/G91I, D195A/G87-88L, E102Q/G91I, and E102Q/G87-88L) prevented their signal detection in PFO-PAGE, despite faint bands in SLS-PAGE (unpublished data). Surprisingly, removing the N-terminal 36 residues (Δ36aa, including the TM region of aa 8–32) of σ_1R resulted in a mutant that showed as a distinct monomer in PFO-PAGE and SLS-PAGE (lane 11, Fig. 6, B and C). The mutant lacking N-terminal 10 residues (Δ10aa) displayed severely impaired oligomerization (lane 16). However, a mutant lacking first five residues (Δ5aa) but sparing the TM substantially retained multimerization (lane 15). Moreover, the E102Q mutant with Δ5aa remained as dimer (lane 14), but was converted to apparent monomer if combined with Δ36aa (lane 13). Similarly, Δ36aa deletion also changed dimeric G91I to monomer (lane 12).

These data suggest that in addition to key residues in the trimerization interface and GXXXG motif, the N-terminal (NT) domain of σ_1R plays a crucial role in its multimerization by potentially linking two homotrimers to form a hexamer or multiple homotrimers to high-order oligomers. In fact, the unit cell organization of σ_1R crystals shows a pair of homotrimers linked together through interactions of two parallel NT domains, each from a protomer of the two neighboring homotrimers (Schmidt et al., 2016). Further evidence was obtained in mutational analysis on σ_1R homomeric interaction by cotransfection of Myc-tagged WT σ_1R and a series of deletion mutants of σ_1R with N-terminal glutathione *S*-transferase fusion. Even upon gradual truncations of more than 100 residues in the C terminus of glutathione *S*-transferase–σ_1R, Myc-σ_1R was coenriched by glutathione beads pull-down. However, this interaction was substantially diminished if the NT of σ_1R was deleted (Supplemental Fig. 4).

Next, the impact of σ_1R oligomerization on ligand binding was studied. GDN-solubilized lysates from FH-σ_1R cells showed robust [^{3}H](+)-pentazocine binding, with a K_d value (37.8 ± 3.3 nM, avg. ± S.E.M.) in a similar range to that of σ_1R expressed in Sf9 cell membranes (Schmidt et al., 2016) and a B_{max} value (20.3 ± 2.3 pmol/mg protein) several-fold higher than those in native tissues (McCann and Su, 1991; Bowen et al., 1993). Remarkably, σ_1R binding exhibited exquisite sensitivity to pH values in the buffer. Compared with normal buffer of pH 7.5, total binding (in the absence of unlabeled ligands) was markedly enhanced in a basic buffer of pH 9 but reduced in an acidic buffer of pH 6 (Fig. 7A). Kinetic analysis of these homologous competition-binding data (Fig. 7B) revealed that in pH 9, there was a significant decrease in K_d value (i.e., increase in affinity) of (+)-pentazocine rather than an increase in binding B_{max} (Fig. 7, C and D). In contrast, acidic buffer (pH 6) significantly decreased not only binding affinity but also B_{max} values of [^{3}H](+)-pentazocine. These changes in ligand binding appeared to correlate with the oligomeric states of σ_1R revealed in PFO-PAGE. Compared with control (pH 7.5), there was a significant increase in σ_1R multimers at pH 9, with a concomitant decrease in dimers and monomers (Fig. 7E). An opposite effect was observed at pH 6. These data suggest that ligand binding to σ_1R is significantly affected by its quaternary structures.

Considering multiple oligomeric states of σ_1R, ideally [^{3}H](+)-pentazocine binding should be analyzed using a multistate model. However, computer-assisted nonlinear regression of binding data showed that a simple, one-site model

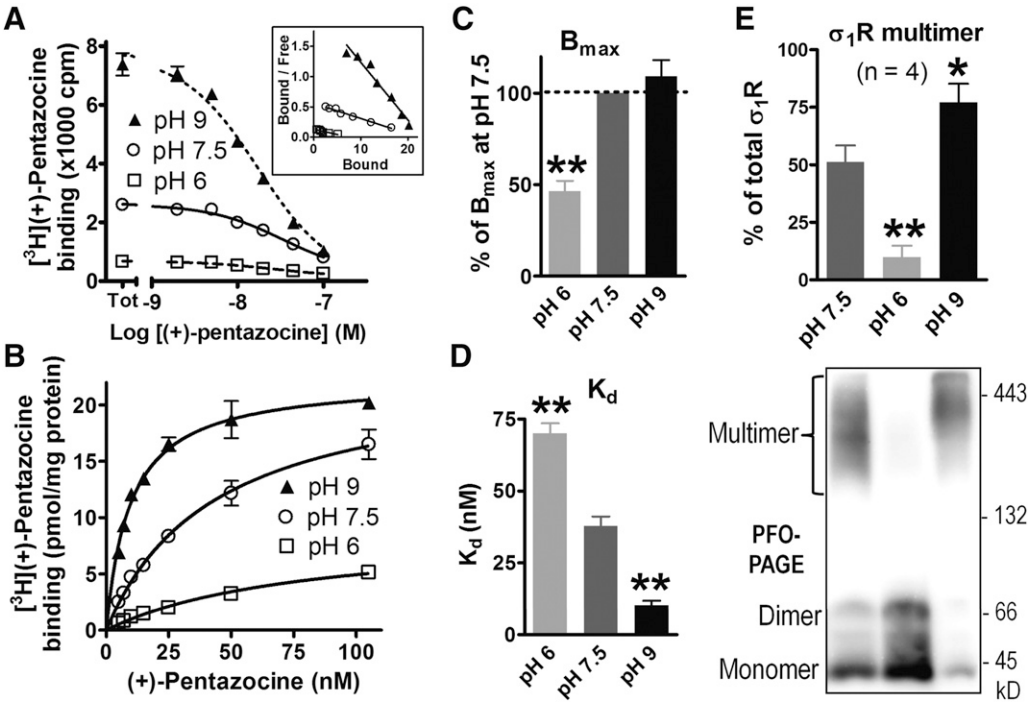

Fig. 7. Correlation of [^{3}H](+)-pentazocine binding with σ_1R quaternary structures in different pH buffers. Lysates from GDN-solubilized FH-σ_1R cells were incubated overnight on ice in Tris buffer of pH 6, 7.5, or 9 and analyzed in binding assays. Representative raw data in (A) (inset shows Scatchard plot) and binding isotherms in (B). Both: duplicate samples (avg. ± S.D.). Tot, total binding. (C and D) Comparisons of B_{max} and K_d values (mean ± S.E.M., $n = 4$ experiments, each with duplicates). (E) Modulation of σ_1R oligomerization by buffer pH values, as examined in PFO-PAGE. Top: graph showing σ_1R multimer band densities as % of total σ_1R (mean ± S.E.M., $n = 4$ experiments) in PFO-PAGE; bottom, representative blot. $^*P < 0.05$; $^{**}P < 0.01$, one-way ANOVA and post hoc Dunnett's test, vs. pH 7.5.

TABLE 1

B_{max} and K_d values of [^{3}H](+)-pentazocine binding in HEK293 stably transfected with σ_1R constructs

B_{max} values were adjusted to total protein concentrations in lysates. Shown values are mean ± S.E.M. from $n = 3$ experiments, each with duplicates except WT ($n = 4$), E102Q, and ΔE3 ($n = 2$). B_{max} of endogenous σ_1R in untransfected HEK293 cells was 2% of that in WT transfected cells and was subtracted from these values. Note small B_{max} values of mutants except Δ36aa were partly attributed to their lower expression levels than WT (Fig. 6). All had N-Myc tag except FH-σ_1R Δ36aa.

	σ_1R					
	WT	Δ36aa	R119A	D195A	E102Q	ΔE3
B_{max} (pmol/mg protein)	16.6 ± 3.5	0.08 ± 0.05	1.83 ± 0.13	3.67 ± 0.26	0.99 ± 0.06	0.21 ± 0.22
K_d (nM)	16.4 ± 7.5	14.0 ± 3.2	9.8 ± 1.4	12.9 ± 2.7	5.0 ± 0.6	17.0 ± 14.1

would suffice (Fig. 7, A and B), and Scatchard plot appeared to be linear (Fig. 7A inset). Statistical comparisons of one-site versus two-site models did not consistently yield clear-cut conclusions.

Reduced capacity to bind [^{3}H](+)-pentazocine were observed in GDN lysates of σ_1R mutants deficient in multimerization, including ΔE3, E102Q, R119A, and D195A (Table 1). B_{max} values measured in untransfected HEK293 cells were negligible (2% of WT σ_1R-transfected cells, in pmol/mg protein), presumably because of a low level of endogenous σ_1R. The weak expression levels of these mutants in transfected cells confounded the interpretation of their low B_{max}. For instance, D195A σ_1R still showed approximately 20% of binding B_{max} of WT σ_1R despite its low expression, suggesting that (+)-pentazocine binding was not fully compromised in this dimer-forming mutant. Nevertheless, the monomer-only mutant Δ36aa σ_1R did not bind (+)-pentazocine, despite its sufficient expression. Together with observations that pH sensitivity of (+)-pentazocine binding correlated with changes of σ_1R multimerization (Fig. 7), these data support the hypothesis that σ_1R multimers exhibit most active conformation for high-affinity (+)-pentazocine binding, whereas its monomers likely do not bind (+)-pentazocine.

Discussion

This study used two nondenaturing gel methods to examine σ_1R oligomerization. In general, agonists decreased σ_1R multimers, whereas antagonists increased multimers (Figs. 1–5). Antagonist binding appeared to stabilize σ_1R multimers, because a higher temperature was required to dissociate σ_1R multimers (Fig. 4).

Although these methods detected multiple high-MM smear bands, they could not determine the stoichiometry of σ_1R multimers. Detergent solubilization might introduce artificial aggregates of σ_1R. However, distinct changes in band signals by ligands argue against this. Furthermore, existence of high-MM σ_1R complex was supported by early purification studies using [^{3}H]azido-DTG or [^{3}H](+)SKF10047 as affinity ligands, in which the labeled protein complex under nondenaturing conditions appeared to be approximately 150 or 450 kDa (Kavanaugh et al., 1988; McCann and Su, 1991). In blue native gels, purified σ_1R showed as multiple smear bands from 60 to 480 kDa (Schmidt et al., 2016).

In rat liver membranes very little dimer and no monomer of σ_1R were present in PFO-PAGE (Fig. 5A), suggesting that native σ_1R multimeric complex was more resistant to extraction by PFO. Distinct drug effects on σ_1R multimerization were optimally demonstrated by SLS-PAGE (Fig. 5C). σ_1R multimers appeared as high-MM bands, including possible trimer, tetramer, and beyond. All σ_1R multimers disappeared in denaturing SDS-PAGE. A weak band of σ_1R trimer was induced by BD1008, if samples were not heated with SDS (Fig. 5B).

Notwithstanding their limitations, these nondenaturing gel approaches offered a relatively straightforward readout of σ_1R oligomerization. Results on G91I mutant were consistent between PFO-PAGE (Fig. 6B) and size-exclusion chromatography (Gromek et al., 2014). Two recent studies used Förster or bioluminescence resonance energy transfer assays to examine ligand effects on σ_1R oligomerization (Mishra et al., 2015; Yano et al., 2018). These assays are advantageous in monitoring the distance between donor- and acceptor-tagged σ_1R in live cells, whereas PFO-PAGE and SLS-PAGE appear to be more sensitive in detecting effects by some ligands, such as BD1047 and DTG.

To induce maximal effects on σ_1R multimerization, most drugs were used at low micromolar concentrations, approximately 100–1000-fold of their K_i values for σ_1R. (+)-Pentazocine showed dose-dependent effects on decreasing σ_1R multimers (Fig. 1C). With a subnanomolar affinity for σ_1R (James et al., 2012), CM304 induced significant effects at 0.1 μM. Although 0.45 μM drugs was sufficient to stabilize oligomers of σ_1R purified from bacteria (Gromek et al., 2014), 100 μM (+)-pentazocine or haloperidol was used in COS-7 cells for Förster resonance energy transfer analysis (Mishra et al., 2015). Thus, higher concentrations of drugs were necessary to permeate across membranes to bind intracellular σ_1R in cells. Most ligands tested here are relatively selective for σ_1R, but haloperidol also has a high affinity for dopamine D_2 receptors. This action was unlikely involved, because haloperidol had effects on σ_1R multimerization in cold cell lysates (Supplemental Fig. 1).

It is worth noting that effects of PRE-084 and NE-100 on σ_1R multimerization did not correlate with their binding affinities. The binding pocket in σ_1R can accommodate diverse ligands with a charged nitrogen as the central pharmacophore (Ablordeppey and Glennon, 2007). Comparison between σ_1R structures bound with (+)-pentazocine and NE-100 revealed limited conformational rearrangement (Schmidt et al., 2018). These structures likely provided snapshots of σ_1R in its lowest free-energy state. However, dynamic conformational changes induced by different ligands and impact on σ_1R quaternary structures have not been thoroughly examined. Further, drug binding to σ_1R may exhibit different cooperativity. Although (+)-pentazocine fully occupied the binding pocket of each σ_1R protomer in crystal structures, binding kinetic analysis of FLAG-tagged σ_1R and molecular dynamics simulation supported a multistep model of (+)-pentazocine binding (Schmidt et al., 2018). Whether PRE-084 or NE-100 induces different conformational changes or binding cooperativity of σ_1R from (+)-pentazocine will require more sophisticated techniques.

Stabilization of σ_1R multimer by antagonists may be explained by their preferential higher affinity for σ_1R multimers rather than dimers/monomers. In WT σ_1R haloperidol's IC_{50} value for competing against [^{3}H](+)-pentazocine binding was approximately one-tenth of those in R119A or D195A mutants (unpublished data), which form only dimers and monomers. However, similar K_d values (Table 1) were not sufficient to explain why (+)-pentazocine dissociated σ_1R multimers. Other potential mechanisms, such as negative protomer cooperativity for (+)-pentazocine binding, will be pursued in future studies.

As σ_1R interacts with many protein partners and regulates their function (Schmidt and Kruse, 2019), efficacies of σ_1R drugs in functional assays are likely determined by multiple factors at molecular, cellular, and higher integrative levels. (+)-Pentazocine decreased σ_1R's association with binding immunoglobin protein (Hayashi and Su, 2007), whereas haloperidol decreased its association with acid-sensing ion channels (Carnally et al., 2010), suggesting that different partners may preferentially interact with specific oligomeric forms of σ_1R. Changes in σ_1R oligomerization by ligands can modulate the availability of σ_1R to associate with its partners, but do not fully account for ligands' efficacies in functional assays.

Data in this study suggest that multiple domains coordinate σ_1R oligomerization. Crystal structures of σ_1R have pinpointed critical residues mediating interactions for homotrimerization (Schmidt et al., 2016). Mutation of Arg119 or Asp195 abolished multimers in nondenaturing gels, confirming a crucial role of hydrogen bonds at these positions. Furthermore, hydrophobic interactions and van der Waals forces involving Phe191 and Trp136 are also pivotal, because removing their aromatic side chains severely impaired multimerization (Fig. 6, B and C). The importance of the GXXXG motif (Gromek et al., 2014) was also substantiated by results of G91I σ_1R in PFO-PAGE. Because Gly91 is in close proximity (4 to 5 Å) to Trp136 of a neighboring protomer in σ_1R crystal structures, mutation to bulky side chain disrupted multimerization.

In nondenaturing gels, multiple high-MM smeared bands appeared larger than σ_1R homotrimers, suggesting possible high-order organization of σ_1R trimers. A corollary of this scenario would require additional domains to mediate noncovalent assembly of trimeric building blocks. Current data support the hypothesis that the NT of σ_1R serves such a role. Unlike WT σ_1R and the Δ5aa mutant, Δ10aa and Δ36aa mutants yielded only monomers in PFO-PAGE (Fig. 6B) despite their intact trimerization domains. It is tempting to speculate that intact NT interactions are required to initiate σ_1R high-order assembly.

This provocative hypothesis is partly corroborated by σ_1R crystal structures, in which each unit cell comprises two pairs of homotrimers (Schmidt et al., 2016). Both pairs are linked together through interactions of two parallel NT domains, each from a protomer in the two homotrimers (Fig. 6A). The opposite orientation of the two pairs requires their embedding into two lipid bilayers in native membranes and is possibly an artifact in crystallization. However, dimerization of homotrimers may resemble a form of native σ_1R oligomerization.

Dimer formation after dissociation of multimers may involve assembly of two protomers from neighboring homotrimers via their NT interactions or rearrangement of two cognate protomers within a homotrimer. Current results on NT truncations favor the first scenario but do not rule out the latter. Dimer interactions appeared to be preserved by PFO but disrupted by the more stringent detergent, SLS. Persistence of E102Q or ΔE3 σ_1R dimers in SLS-PAGE is perplexing and requires further investigation. The E102Q mutant was shown to be prone to aggregation and have aberrant cellular location (Wong et al., 2016; Dreser et al., 2017). In coimmunoprecipitation assays, ΔE3 σ_1R exhibited altered association with the dopamine transporter, compared with WT σ_1R (Hong et al., 2017), and exerted dominant-negative effects in disrupting association of WT σ_1R with μ opioid receptors (Pan et al., 2017). These results suggest that dysregulation of σ_1R quaternary structure impairs its physiologic function.

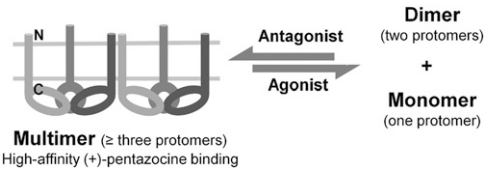

Fig. 8. Hypothesis cartoon based on results in this study and previous reports. Agonists and antagonists differentially affect σ_1R multimerization. High-order organization of σ_1R likely comprises multiple (≥2) units of homotrimers. Current data suggest a critical role of the N terminus in mediating formation of multimers beyond homotrimers.

Intriguingly, buffer pH significantly altered the oligomeric states of σ_1R (Fig. 7E). Although the underlying mechanism and physiologic significance are beyond the scope of this study, a rudimentary inference is that σ_1R multimers dissociate in acidic lysosomes to facilitate degradation. This serendipitous finding helps to examine how σ_1R oligomerization affected ligand binding. Results (Fig. 7) indicate that σ_1R multimers possess high-affinity and high-capacity binding of [^{3}H](+)-pentazocine. Because Δ36aa σ_1R formed monomer exclusively but lacked binding (Table 1), it was inferred that monomeric σ_1R could not bind (+)-pentazocine. This hypothesis is consistent with a previous study using σ_1R mutants from bacterial expression (Gromek et al., 2014).

In summary, this study demonstrated that multiple domains coordinate the oligomerization of σ_1R. The equilibrium between monomers, dimers, and multimers of σ_1R is dynamically regulated by agonists or antagonists in distinct manners. Antagonists promote σ_1R multimerization, whereas agonists facilitate its dissociation (Fig. 8). σ_1R mutants implicated in neurodegenerative diseases displayed aberrant multimerization, suggesting that balance in σ_1R oligomerization is important in its physiologic function. Extensive studies have shown that σ_1R associates with a plethora of partner proteins that are involved in diverse cellular signaling pathways. Distinct regulation of σ_1R multimerization by agonists and antagonists may selectively modulate activities of clientele proteins within their interactome network. Future work will shed light on whether σ_1R oligomerization may be precisely controlled by cells' adaptive responses to physiochemical changes in the environment, which in turn may impact these signaling mechanisms.

Acknowledgments

I thank Drs. Jonathan L. Katz, Mark R. Macbeth, Jie Jiang, and Alex Erkine for advice and comments on this manuscript; I am grateful for the generous gifts of various σ_1R ligands from Jonathan

L. Katz, Christopher R. McCurdy, and National Institute on Drug Abuse (NIDA) Drug Supply Program.

Authorship Contributions

Participated in research design: Hong.
Conducted experiments: Hong.
Performed data analysis: Hong.
Wrote or contributed to the writing of the manuscript: Hong.

References

Ablordeppey SY and Glennon RA (2007) Pharmacophore models for sigma-1 receptor binding, in *Sigma Receptors: Chemistry, Cell Biology and Clinical Implications* (Matsumoto RR, Bowen WD, and Su TP 71–98, Springer, New York.

Al-Saif A, Al-Mohanna F, and Bohlega S (2011) A mutation in sigma-1 receptor causes juvenile amyotrophic lateral sclerosis. *Ann Neurol* **70**:913–919.

Aydar E, Palmer CP, Klyachko VA, and Jackson MB (2002) The sigma receptor as a ligand-regulated auxiliary potassium channel subunit. *Neuron* **34**:399–410.

Balasuriya D, Stewart AP, Crottès D, Borgese F, Soriani O, and Edwardson JM (2012) The sigma-1 receptor binds to the Nav1.5 voltage-gated Na+ channel with 4-fold symmetry. *J Biol Chem* **287**:37021–37029.

Bergeron R, de Montigny C, and Debonnel G (1996) Potentiation of neuronal NMDA response induced by dehydroepiandrosterone and its suppression by progesterone: effects mediated via sigma receptors. *J Neurosci* **16**:1193–1202.

Bernard-Marissal N, Médard JJ, Azzedine H, and Chrast R (2015) Dysfunction in endoplasmic reticulum-mitochondria crosstalk underlies SIGMAR1 loss of function mediated motor neuron degeneration. *Brain* **138**:875–890.

Bowen WD, de Costa BR, Hellwell SB, Walker JM, and Rice KC (1993) [^{3}H]-(+) Pentazocine: a potent and highly selective benzomorphan-based probe for sigma-1 receptors. *Mol Neuropharmacol* **3**:117–126.

Cai Y, Yang L, Niu F, Liao K, and Buch S (2017) Role of sigma-1 receptor in cocaine Abuse and neurodegenerative disease, in *Sigma Receptors: Their Role in Disease and as Therapeutic Targets* (Smith SB and Su T-P 163–175, Springer International Publishing, Cham, Switzerland.

Carnally SM, Johannessen M, Henderson RM, Jackson MB, and Edwardson JM (2010) Demonstration of a direct interaction between sigma-1 receptors and acid-sensing ion channels. *Biophys J* **98**:1182–1191.

Chu UB and Ruoho AE (2016) Biochemical pharmacology of the sigma-1 receptor. *Mol Pharmacol* **89**:142–153.

Cobos EJ, Entrena JM, Nieto FR, Cendán CM, and Del Pozo E (2008) Pharmacology and therapeutic potential of sigma(1) receptor ligands. *Curr Neuropharmacol* **6**: 344–366.

Dreser A, Vollrath JT, Sechi A, Johann S, Roos A, Yamoah A, Katona I, Bohlega S, Wiemuth D, Tian Y, et al. (2017) The ALS-linked E102Q mutation in Sigma receptor-1 leads to ER stress-mediated defects in protein homeostasis and dysregulation of RNA-binding proteins. *Cell Death Differ* **24**:1655–1671.

Fontanilla D, Johannessen M, Hajipour AR, Cozzi NV, Jackson MB, and Ruoho AE (2009) The hallucinogen N,N-dimethyltryptamine (DMT) is an endogenous sigma-1 receptor regulator. *Science* **323**:934–937.

Francardo V, Bez F, Wieloch T, Nissbrandt H, Ruscher K, and Cenci MA (2014) Pharmacological stimulation of sigma-1 receptors has neurorestorative effects in experimental parkinsonism. *Brain* **137**:1998–2014.

Ganapathy ME, Prasad PD, Huang W, Seth P, Leibach FH, and Ganapathy V (1999) Molecular and ligand-binding characterization of the sigma-receptor in the Jurkat human T lymphocyte cell line. *J Pharmacol Exp Ther* **289**:251–260.

Gregianin E, Pallafacchina G, Zanin S, Crippa V, Rusmini P, Poletti A, Fang M, Li Z, Diano L, Petrucci A, et al. (2016) Loss-of-function mutations in the SIGMAR1 gene cause distal hereditary motor neuropathy by impairing ER-mitochondria tethering and Ca^{2+} signalling. *Hum Mol Genet* **25**:3741–3753.

Gromek KA, Suchy FP, Meddaugh HR, Wrobel RL, LaPointe LM, Chu UB, Primm JG, Ruoho AE, Senes A, and Fox BG (2014) The oligomeric states of the purified sigma-1 receptor are stabilized by ligands. *J Biol Chem* **289**:20333–20344.

Hanner M, Moebius FF, Flandorfer A, Knaus HG, Striessnig J, Kempner E, and Glossmann H (1996) Purification, molecular cloning, and expression of the mammalian sigma1-binding site. *Proc Natl Acad Sci USA* **93**:8072–8077.

Hayashi T and Su TP (2001) Regulating ankyrin dynamics: roles of sigma-1 receptors. *Proc Natl Acad Sci USA* **98**:491–496.

Hayashi T and Su TP (2007) Sigma-1 receptor chaperones at the ER-mitochondrion interface regulate Ca^{2+} signaling and cell survival. *Cell* **131**:596–610.

Hiranita T, Soto PL, Kohut SJ, Kopajtic T, Cao J, Newman AH, Tanda G, and Katz JL (2011) Decreases in cocaine self-administration with dual inhibition of the dopamine transporter and σ receptors. *J Pharmacol Exp Ther* **339**:662–677.

Hong WC, Yano H, Hiranita T, Chin FT, McCurdy CR, Su TP, Amara SG, and Katz JL (2017) The sigma-1 receptor modulates dopamine transporter conformation and cocaine binding and may thereby potentiate cocaine self-administration in rats. *J Biol Chem* **292**:11250–11261.

James ML, Shen B, Zavaleta CL, Nielsen CH, Mesangeau C, Vuppala PK, Chan C, Avery BA, Fishback JA, Matsumoto RR, et al. (2012) New positron emission tomography (PET) radioligand for imaging σ-1 receptors in living subjects. *J Med Chem* **55**:8272–8282.

Jbilo O, Vidal H, Paul R, De Nys N, Bensaid M, Silve S, Carayon P, Davi D, Galiègue S, Bourrié B, et al. (1997) Purification and characterization of the human SR 31747A-binding protein. A nuclear membrane protein related to yeast sterol isomerase. *J Biol Chem* **272**:27107–27115.

Katz JL, Hiranita T, Hong WC, Job MO, and McCurdy CR (2017) A role for sigma receptors in stimulant self-administration and addiction. *Handb Exp Pharmacol* **244**:177–218.

Kavanaugh MP, Tester BC, Scherz MW, Keana JF, and Weber E (1988) Identification of the binding subunit of the sigma-type opiate receptor by photoaffinity labeling with 1-(4-azido-2-methyl[6-3H]phenyl)-3-(2-methyl[4,6-3H]phenyl)guanidine. *Proc Natl Acad Sci USA* **85**:2844–2848.

Kim FJ, Kovalyshyn I, Burgman M, Neilan C, Chien CC, and Pasternak GW (2010) Sigma 1 receptor modulation of G-protein-coupled receptor signaling: potentiation of opioid transduction independent from receptor binding. *Mol Pharmacol* **77**: 695–703.

Kourrich S, Hayashi T, Chuang JY, Tsai SY, Su TP, and Bonci A (2013) Dynamic interaction between sigma-1 receptor and Kv1.2 shapes neuronal and behavioral responses to cocaine. *Cell* **152**:236–247.

Lahmy V, Meunier J, Malmstrom S, Naert G, Givalois L, Kim SH, Villard V, Vamvakides A, and Maurice T (2013) Blockade of Tau hyperphosphorylation and $A\beta_{1-42}$ generation by the aminotetrahydrofuran derivative ANAVEX2-73, a mixed muscarinic and σ_1 receptor agonist, in a nontransgenic mouse model of Alzheimer's disease. *Neuropsychopharmacology* **38**:1706–1723.

Li X, Hu Z, Liu L, Xie Y, Zhan Y, Zi X, Wang J, Wu L, Xia K, Tang B, et al. (2015) A SIGMAR1 splice-site mutation causes distal hereditary motor neuropathy. *Neurology* **84**:2430–2437.

Martin WR, Eades CG, Thompson JA, Huppler RE, and Gilbert PE (1976) The effects of morphine- and nalorphine- like drugs in the nondependent and morphine-dependent chronic spinal dog. *J Pharmacol Exp Ther* **197**:517–532.

Matsumoto RR (2007) Sigma receptors: historical perspective and background, in *Sigma Receptors: Chemistry, Cell Biology and Clinical Implications* (Matsumoto RR, Bowen WD, and Su TP 1–24, Springer, New York.

Maurice T and Goguadze N (2017) Sigma-1 (σ_1) receptor in memory and neurodegenerative diseases. *Handb Exp Pharmacol* **244**:81–108.

Maurice T and Su TP (2009) The pharmacology of sigma-1 receptors. *Pharmacol Ther* **124**:195–206.

McCann DJ and Su TP (1991) Solubilization and characterization of haloperidol-sensitive (+)-[^{3}H]SKF-10,047 binding sites (sigma sites) from rat liver membranes. *J Pharmacol Exp Ther* **257**:547–554.

Merlos M, Romero L, Zamanillo D, Plata-Salamán C, and Vela JM (2017) Sigma-1 receptor and pain. *Handb Exp Pharmacol* **244**:131–161.

Mishra AK, Mavlyutov T, Singh DR, Biener G, Yang J, Oliver JA, Ruoho A, and Raicu V (2015) The sigma-1 receptors are present in monomeric and oligomeric forms in living cells in the presence and absence of ligands. *Biochem J* **466**:263–271.

Navarro G, Moreno E, Aymerich M, Marcellino D, McCormick PJ, Mallol J, Cortés A, Casadó V, Canela EI, Ortiz J, et al. (2010) Direct involvement of sigma-1 receptors in the dopamine D1 receptor-mediated effects of cocaine. *Proc Natl Acad Sci USA* **107**:18676–18681.

Newman AH and Coop A (2007) Medicinal chemistry: new chemical classes and subtype-selective ligands, in *Sigma Receptors: Chemistry, Cell Biology and Clinical Implications* (Matsumoto RR, Bowen WD, and Su TP 25–44, Springer, New York.

Ortega-Roldan JL, Ossa F, and Schnell JR (2013) Characterization of the human sigma-1 receptor chaperone domain structure and binding immunoglobulin protein (BiP) interactions. *J Biol Chem* **288**:21448–21457.

Pan L, Pasternak DA, Xu J, Xu M, Lu Z, Pasternak GW, and Pan YX (2017) Isolation and characterization of alternatively spliced variants of the mouse sigma1 receptor gene, Sigmar1. *PLoS One* **12**:e0174694.

Penna A, Demuro A, Yeromin AV, Zhang SL, Safrina O, Parker I, and Cahalan MD (2008) The CRAC channel consists of a tetramer formed by Stim-induced dimerization of Orai dimers. *Nature* **456**:116–120.

Ramachandran S, Chu UB, Mavlyutov TA, Pal A, Pyne S, and Ruoho AE (2009) The sigma1 receptor interacts with N-alkyl amines and endogenous sphingolipids. *Eur J Pharmacol* **609**:19–26.

Ramjeesingh M, Huan LJ, Garami E, and Bear CE (1999) Novel method for evaluation of the oligomeric structure of membrane proteins. *Biochem J* **342**:119–123.

Reichel C (2012) SARCOSYL-PAGE: a new electrophoretic method for the separation and immunological detection of PEGylated proteins. *Methods Mol Biol* **869**:65–79.

Robson MJ, Turner RC, Naser ZJ, McCurdy CR, O'Callaghan JP, Huber JD, and Matsumoto RR (2014) SN79, a sigma receptor antagonist, attenuates methamphetamine-induced astrogliosis through a blockade of OSMR/gp130 signaling and STAT3 phosphorylation. *Exp Neurol* **254**:180–189.

Ryskamp D, Wu J, Geva M, Kusko R, Grossman I, Hayden M, and Bezprozvanny I (2017) The sigma-1 receptor mediates the beneficial effects of pridopidine in a mouse model of Huntington disease. *Neurobiol Dis* **97** (Pt A):46–59.

Ryskamp D, Wu L, Wu J, Kim D, Rammes G, Geva M, Hayden M, and Bezprozvanny I (2019) Pridopidine stabilizes mushroom spines in mouse models of Alzheimer's disease by acting on the sigma-1 receptor. *Neurobiol Dis* **124**:489–504.

Sabino V and Cottone P (2017) Sigma receptors and alcohol use disorders. *Handb Exp Pharmacol* **244**:219–236.

Sambo DO, Lin M, Owens A, Lebowitz JJ, Richardson B, Jagnarine DA, Shetty M, Rodriquez M, Alonge T, Ali M, et al. (2017) The sigma-1 receptor modulates methamphetamine dysregulation of dopamine neurotransmission. *Nat Commun* **8**: 2228.

Schmidt HR, Betz RM, Dror RO, and Kruse AC (2018) Structural basis for σ_1 receptor ligand recognition. *Nat Struct Mol Biol* **25**:981–987.

Schmidt HR and Kruse AC (2019) The molecular function of σ receptors: past, present, and future. *Trends Pharmacol Sci* **40**:636–654.

Schmidt HR, Zheng S, Gurpinar E, Koehl A, Manglik A, and Kruse AC (2016) Crystal structure of the human σ1 receptor. *Nature* **532**:527–530.

Srivats S, Balasuriya D, Pasche M, Vistal G, Edwardson JM, Taylor CW, and Murrell-Lagnado RD (2016) Sigma1 receptors inhibit store-operated Ca^{2+} entry by attenuating coupling of STIM1 to Orai1. *J Cell Biol* **213**:65–79.

Su TP, London ED, and Jaffe JH (1988) Steroid binding at sigma receptors suggests a link between endocrine, nervous, and immune systems. *Science* **240**:219–221.

Thomas JD, Longen CG, Oyer HM, Chen N, Maher CM, Salvino JM, Kania B, Anderson KN, Ostrander WF, Knudsen KE, et al. (2017) Sigma1 targeting to

suppress aberrant androgen receptor signaling in prostate cancer. *Cancer Res* **77**: 2439–2452.
Walker JM, Bowen WD, Walker FO, Matsumoto RR, De Costa B, and Rice KC (1990) Sigma receptors: biology and function. *Pharmacol Rev* **42**:355–402.
Wang J, Saul A, Roon P, and Smith SB (2016) Activation of the molecular chaperone, sigma 1 receptor, preserves cone function in a murine model of inherited retinal degeneration. *Proc Natl Acad Sci USA* **113**:E3764–E3772.
Watanabe S, Ilieva H, Tamada H, Nomura H, Komine O, Endo F, Jin S, Mancias P, Kiyama H, and Yamanaka K (2016) Mitochondria-associated membrane collapse is a common pathomechanism in SIGMAR1- and SOD1-linked ALS. *EMBO Mol Med* **8**:1421–1437.
Weber F and Wünsch B (2017) Medicinal chemistry of σ_1 receptor ligands: pharmacophore models, synthesis, structure affinity relationships, and pharmacological applications. *Handb Exp Pharmacol* **244**:51–79.
Wong AY, Hristova E, Ahlskog N, Tasse LA, Ngsee JK, Chudalayandi P, and Bergeron R (2016) Aberrant subcellular dynamics of sigma-1 receptor mutants underlying neuromuscular diseases. *Mol Pharmacol* **90**:238–253.
Wu Z and Bowen WD (2008) Role of sigma-1 receptor C-terminal segment in inositol 1,4,5-trisphosphate receptor activation: constitutive enhancement of calcium signaling in MCF-7 tumor cells. *J Biol Chem* **283**:28198–28215.
Yano H, Bonifazi A, Xu M, Guthrie DA, Schneck SN, Abramyan AM, Fant AD, Hong WC, Newman AH, and Shi L (2018) Pharmacological profiling of sigma 1 receptor ligands by novel receptor homomer assays. *Neuropharmacology* **133**:264–275.

Address correspondence to: Dr. Weimin Conrad Hong, Department of Pharmaceutical Sciences, Butler University, PB351, 4600 Sunset Ave., Indianapolis, IN 46208. E-mail: chong@butler.edu